PHYSICAL REVIEW D **94,** 065010 (2016)

Mirror reflections of a black hole

Michael R. R. Good[*]
Department of Physics, Nazarbayev University, Astana 010000, Kazakhstan

Paul R. Anderson[†]
Department of Physics, Wake Forest University, Winston-Salem, North Carolina 27109, USA

Charles R. Evans[‡]
Department of Physics and Astronomy, University of North Carolina at Chapel Hill, North Carolina 27514, USA

(Received 21 May 2016; published 12 September 2016)

An exact correspondence between a black hole and an accelerating mirror is demonstrated. It is shown that for a massless minimally coupled scalar field, the same Bogolubov coefficients connecting the "in" and "out" states occur for a $(1+1)$-dimensional flat spacetime with a particular perfectly reflecting accelerating boundary trajectory and a $(1+1)$-dimensional curved spacetime in which a null shell collapses to form a black hole. Generalization of the latter to the $(3+1)$-dimensional case is discussed. The spectral dynamics is computed in both $(1+1)$-dimensional spacetimes along with the energy flux in the spacetime with a mirror. It is shown that the approach to equilibrium is monotonic, asymmetric in terms of the rate, and there is a specific time which characterizes the system when it is the most out of equilibrium.

DOI: 10.1103/PhysRevD.94.065010

I. INTRODUCTION

The connection between the particle production which occurs at late times after a black hole forms from collapse [1] and the late-time particle production from a mirror in flat space that accelerates without bound, asymptotically approaching a null geodesic, was established by Davies and Fulling [2,3]. An interesting question is whether there are mirror trajectories for which their entire history of particle creation, from initial nonthermal phase to late-time thermal emission, corresponds to the entire history of particle creation from a spacetime in which a black hole forms from collapse. We have found a specific example in $(1+1)$ dimensions where there is such an exact correspondence.

The model for gravitational collapse that we consider consists of a collapsing shell with a null trajectory. The spacetime inside the shell is flat, while the geometry outside the shell is the usual Schwarzschild geometry. This model was considered in [4] where the exact Bogolubov coefficients connecting the "in" and "out" vacuum states were computed for a massless minimally coupled scalar field. The trajectory for the mirror is a simple modification of one that was discovered in Ref. [5]. The mirror, which is in flat space, begins at past timelike infinity, i^-, and accelerates in a monotonic fashion, asymptotically approaching $v = v_H$ with $v \equiv t + r$.

One of the advantages of our model is that the Bogolubov coefficients between the "in" and "out" states can be computed analytically. It is the equivalence between these coefficients in the black hole and accelerating mirror cases that establishes the exact connection. Interestingly, in the mirror case, there are so far a limited number of specific trajectories for which the Bogolubov coefficients have been computed analytically [3,6–9]. In most of these cases, as in the present case, the actual amount of particle production must be computed numerically.

In [10–12], we pointed out this mirror–black hole connection and briefly explored the time dependence of the particle production and the time dependence of the stress-energy tensor in the accelerating mirror case. Here we give the details of the computations of the Bogolubov coefficients in both the black hole and accelerating mirror cases. For the black hole, we add a discussion of the computation in $(3+1)$ dimensions. We also give a significantly more detailed description of the time dependence of the particle production process, which includes an estimate, consistent with the uncertainty relation, of the time evolution of the spectrum of the produced particles. The time dependence of the particle production process was investigated for other mirror trajectories in [8].

In Sec. II, we compute the Bogolubov coefficients for our mirror trajectory and for the case of a null shell that collapses to form a black hole in $(1+1)$ and $(3+1)$ dimensions. In the latter case, we ignore the effective potential in the mode equation. In Sec. III, the time dependence of the particle production process and the frequency spectrum of the produced particles are investigated. Section IV contains a brief discussion of the time dependence of the stress energy of the quantum field

[*]michael.good@nu.edu.kz
[†]anderson@wfu.edu
[‡]evans@physics.unc.edu

in the accelerating mirror case. Our results are summarized in Sec. V. Throughout, we use units such that $\hbar = c = G = k_B = 1$, and our conventions are those of Ref. [13].

II. BOGOLUBOV COEFFICIENTS

In this section, we compute the particle production that occurs for a massless minimally coupled scalar field in three different situations: a $(1+1)$-dimensional flat spacetime with an accelerating mirror moving along a particular trajectory, a $(1+1)$-dimensional spacetime in which a null shell collapses to form a black hole, and a $(3+1)$-dimensional spherically symmetric spacetime in which a null shell collapses to form a black hole. We begin with the simplest case which is the accelerating mirror.

A. $(1+1)$-dimensional flat spacetime with a mirror

The line element for flat space in $(1+1)$ dimensions is simply

$$ds^2 = -dt^2 + dr^2 = -dudv, \tag{2.1}$$

where alternative, null coordinates are

$$u = t - r, \qquad v = t + r. \tag{2.2}$$

We denote the trajectory of the mirror by $r = z(t)$ (see Fig. 1). Note that we shall only be concerned with the part of the spacetime that is to the right of the mirror.

The wave equation for the massless minimally coupled scalar field is

$$\Box\phi = 0. \tag{2.3}$$

The field can be expanded in terms of complete sets of mode functions, each of which satisfies the equation

$$\partial_u\partial_v f = 0. \tag{2.4}$$

The general solution is

$$f = a(u) + b(v), \tag{2.5}$$

for arbitrary functions a and b.

The modes are normalized using the scalar product

$$\begin{aligned}(\phi_1,\phi_2) &= -i\int_\Sigma d\Sigma\sqrt{|g_\Sigma|}n^a\phi_1\overleftrightarrow{\partial}_a\phi_2^*,\\ &= -i\int_\Sigma d\Sigma\sqrt{|g_\Sigma|}n^a[\phi_1\partial_a\phi_2^* - (\partial_a\phi_1)\phi_2^*],\end{aligned} \tag{2.6}$$

with Σ a Cauchy surface and n^a the unit normal to that surface. One Cauchy surface we shall use is $\mathcal{I}_R^-$. In this case, the scalar product is

$$(\phi_1,\phi_2) = -i\int_{-\infty}^{\infty} dv\phi_1\overleftrightarrow{\partial}_v\phi_2^*. \tag{2.7}$$

The other consists of the union of $\mathcal{I}_R^+$ with $\mathcal{I}_{L,>}^+$, the part of $\mathcal{I}_L^+$ that is to the right of the mirror. The scalar product is then

$$(\phi_1,\phi_2) = -i\int_{-\infty}^{\infty} du\phi_1\overleftrightarrow{\partial}_u\phi_2^* - i\int_{v_H}^{\infty} dv\phi_1\overleftrightarrow{\partial}_v\phi_2^*. \tag{2.8}$$

The "in" modes are normalized on $\mathcal{I}_R^-$ and form a complete set for the region to the right of the mirror. The other set of modes of interest are those which are normalized on $\mathcal{I}_R^+$ and which vanish on $\mathcal{I}_{L,>}^+$. We label these as "out" modes. Another set of modes, labeled "left" modes, end on $\mathcal{I}_{L,>}^+$. Taken together the "out" modes and "left" modes form a complete set. All modes in either set that impinge upon the mirror must vanish at its surface. The "in" and "out" modes thus have the forms

$$f_\omega^{\text{in}} = \frac{1}{\sqrt{4\pi\omega}}[e^{-i\omega v} - e^{-i\omega p(u)}], \tag{2.9a}$$

$$f_\omega^{\text{out}} = \frac{1}{\sqrt{4\pi\omega}}[e^{-i\omega h(v)}\theta(v_H - v) - e^{-i\omega u}], \tag{2.9b}$$

where the ray tracing functions $p(u)$ and $h(v)$ are defined so that at the location of the mirror $p(u) = v$ and $h(v) = u$. See Ref. [8] for details.[1]

To find the number of particles produced, we first expand the field in terms of both sets of modes:

$$\phi = \int_0^\infty d\omega[a_\omega^{\text{in}}f_\omega^{\text{in}} + a_\omega^{\text{in}\dagger}f_\omega^{\text{in}*}], \tag{2.10a}$$

$$= \int_0^\infty d\omega[a_\omega^{\text{out}}f_\omega^{\text{out}} + a_\omega^{\text{out}\dagger}f_\omega^{\text{out}*} + a_\omega^{\text{left}}f_\omega^{\text{left}} + a_\omega^{\text{left}\dagger}f_\omega^{\text{left}*}]. \tag{2.10b}$$

We also write

$$f_\omega^{\text{out}} = \int_0^\infty d\omega'[\alpha_{\omega\omega'}f_{\omega'}^{\text{in}} + \beta_{\omega\omega'}f_{\omega'}^{\text{in}*}]. \tag{2.11}$$

Then using the fact that the modes are orthonormal with respect to the scalar product, one finds that

$$\alpha_{\omega\omega'} = (f_\omega^{\text{out}}, f_{\omega'}^{\text{in}}), \tag{2.12a}$$

$$\beta_{\omega\omega'} = -(f_\omega^{\text{out}}, f_{\omega'}^{\text{in}*}), \tag{2.12b}$$

[1]Note that in [8] the function we call $h(v)$ is denoted by $f(v)$.

$$a_\omega^{\rm out} = (\phi, f_\omega^{\rm out}) = \int_0^\infty d\omega' [a_{\omega'}^{\rm in} \alpha^*_{\omega\omega'} - a_{\omega'}^{\rm in\dagger} \beta^*_{\omega\omega'}]. \quad (2.12c)$$

Then, if the field is in the "in" state, the average number of particles found at $\mathscr{I}^+$ with frequency ω is

$$\langle in | N_\omega^{\rm out} | in \rangle = \int_0^\infty d\omega' |\beta_{\omega\omega'}|^2. \quad (2.13)$$

We now introduce a specific mirror trajectory that begins at past timelike infinity, i^-, and is asymptotic to the ray $v = v_H$. A Penrose diagram for it is given in Fig. 1. The trajectory, which is a slight modification of what was called the Omex trajectory in Ref. [5], is

$$z(t) = v_H - t - \frac{W(2e^{2\kappa(v_H - t)})}{2\kappa}, \quad (2.14)$$

with κ and v_H constants, and with W the Lambert W (or product log) function, which has the properties

$$z = W(z) e^{W(z)} = W(z e^z). \quad (2.15)$$

Then, writing

$$v = v_m(t) = t + z(t), \quad (2.16)$$

with $v_m(t)$ being the value of v for the mirror's location at time t, we find

$$\tilde{t}_m(v) = v - \frac{1}{2\kappa} \log[\kappa(v_H - v)], \quad (2.17)$$

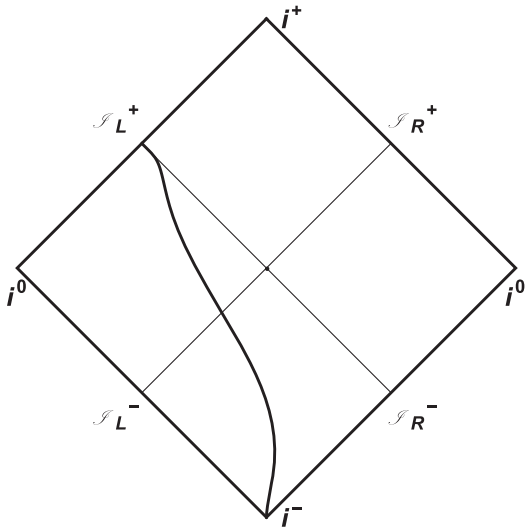

FIG. 1. Penrose diagram for a flat $(1+1)$-dimensional spacetime containing an accelerating mirror with the trajectory (2.14) in the case that $\kappa = 1$ and $v_H = 0$. The trajectory is timelike, begins at i^-, and asymptotically approaches $v = v_H = 0$.

with $\tilde{t}_m(v)$ the time when the mirror intersects the null ray labeled by v. This equation can easily be verified by substituting (2.14) into (2.16) and using (2.17) along with the second relation in (2.15). Then since $h(v) = u$ at the surface of the mirror,

$$h(v) = \tilde{t}_m(v) - z[\tilde{t}_m(v)] = v - \frac{1}{\kappa} \log[\kappa(v_H - v)]. \quad (2.18)$$

The relation $p(u) = v$ which is valid at the surface of the mirror is the inverse of the relation $h(v) = u$. We find that

$$p(u) = v_H - \frac{1}{\kappa} W(e^{-\kappa(u - v_H)}). \quad (2.19)$$

This can be verified by computing $h(p(u))$ and using the first relation in (2.15). Combining the equations $p(u) = v_m = t_m(u) + z[t_m(u)]$ and $t_m(u) = u + z[t_m(u)]$, one finds

$$t_m(u) = \frac{1}{2}\left[v_H + u - \frac{1}{\kappa} W(e^{-\kappa(u - v_H)}) \right]. \quad (2.20)$$

Here $t_m(u)$ is the time when the mirror intersects the null ray labeled by u.

To evaluate the formulas for the Bogolubov coefficients in (2.12a) and (2.12b), we choose the surface $\mathscr{I}_R^-$ for which the general form of the scalar product is given in (2.7). Combining these equations along with (2.9b) and (2.18) and noting that $u = -\infty$ on $\mathscr{I}_R^-$, we find after some algebra that

$$\alpha_{\omega\omega'} = \frac{1}{4\pi} \int_{-\infty}^{v_H} dv e^{-i(\omega - \omega')v} [\kappa(v_H - v)]^{i\omega/\kappa} \times \left\{ \sqrt{\frac{\omega'}{\omega}} + \sqrt{\frac{\omega}{\omega'}} \left[1 + \frac{1}{\kappa(v_H - v)} \right] \right\}, \quad (2.21a)$$

$$\beta_{\omega\omega'} = \frac{1}{4\pi} \int_{-\infty}^{v_H} dv e^{-i(\omega + \omega')v} [\kappa(v_H - v)]^{i\omega/\kappa} \times \left\{ \sqrt{\frac{\omega'}{\omega}} - \sqrt{\frac{\omega}{\omega'}} \left[1 + \frac{1}{\kappa(v_H - v)} \right] \right\}. \quad (2.21b)$$

Changing the integration variable to $x = v_H - v$ allows for the evaluation of the integrals in terms of gamma functions. After more algebra, we find

$$\alpha_{\omega\omega'} = -\frac{e^{-i(\omega - \omega')v_H}}{2\pi\kappa} \frac{\sqrt{\omega\omega'}}{\omega - \omega'} \left[-\frac{i}{\kappa}(\omega - \omega') \right]^{-i\omega/\kappa} \Gamma\left(\frac{i\omega}{\kappa} \right), \quad (2.22a)$$

$$\beta_{\omega\omega'} = -\frac{e^{-i(\omega + \omega')v_H}}{2\pi\kappa} \frac{\sqrt{\omega\omega'}}{\omega + \omega'} \left[-\frac{i}{\kappa}(\omega + \omega') \right]^{-i\omega/\kappa} \Gamma\left(\frac{i\omega}{\kappa} \right). \quad (2.22b)$$

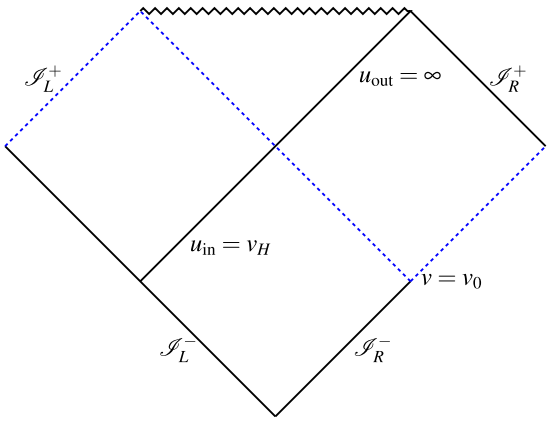

FIG. 2. Penrose diagram for a two-dimensional black hole that forms from the collapse of a null shell along the trajectory $v = v_0$. The Cauchy surface used to compute the Bogolubov coefficients is the dotted (blue) surface formed from $\mathscr{I}_L^+$, part of $\mathscr{I}_R^-$, and the $v = v_0$ null ray. Note that the horizon is the future light cone of the point $(u_{\rm in} = v_H \equiv v_0 - 4M,\ v = v_0)$.

B. (1 + 1)-dimensional spacetime with a collapsing null shell

For a $(1+1)$-dimensional spacetime with a collapsing null shell, the line element inside the shell is still given by (2.1), while outside the shell it is

$$ds^2 = -\left(1 - \frac{2M}{r}\right)dt_s^2 + \left(1 - \frac{2M}{r}\right)^{-1} dr^2. \tag{2.23}$$

The Penrose diagram is given in Fig. 2. We define the usual radial null coordinates inside the shell to be those in Eq. (2.2). Outside both the shell and the horizon, the corresponding coordinates are

$$u_s \equiv t_s - r_*, \tag{2.24a}$$

$$v \equiv t_s + r_*, \tag{2.24b}$$

$$r_* \equiv r + 2M \log\left(\frac{r - 2M}{2M}\right). \tag{2.24c}$$

Following [4,14], we match the coordinate systems along the part of the trajectory of the shell which is outside the horizon in such a way that both v and r are continuous across the surface and $v = v_0$ on the surface. This is why we have no subscripts for these two coordinates. The coordinates t and u are not continuous across the surface. To find the relation between u_s and u, we note that at the surface and outside the event horizon,

$$r = \frac{1}{2}(v_0 - u), \tag{2.25a}$$

$$r_* = \frac{1}{2}(v_0 - u_s) = r + 2M \log\left(\frac{r - 2M}{2M}\right). \tag{2.25b}$$

Substituting (2.25a) into the right-hand side of (2.25b) and solving for u_s gives

$$u_s = u - 4M \log\left(\frac{v_H - u}{4M}\right), \tag{2.26}$$

with

$$v_H \equiv v_0 - 4M. \tag{2.27}$$

Note that the event horizon ($u_s = \infty$) is at $u = v_H$.

We next show that it is possible to invert (2.26) using the Lambert W function. First it is easy to show that (2.26) can be written in the form

$$\exp\left(\frac{v_H - u_s}{4M}\right) = \left(\frac{v_H - u}{4M}\right)\exp\left(\frac{v_H - u}{4M}\right). \tag{2.28}$$

Then computing the Lambert W function of both sides of the equation and using the second relation in (2.15), we find that

$$u = v_H - 4MW\left[\exp\left(\frac{v_H - u_s}{4M}\right)\right]. \tag{2.29}$$

The field ϕ and its mode functions f are solutions to Eq. (2.3). In the flat space region below the null shell, the general solution is (2.5). In the Schwarzschild region above the shell, Eq. (2.3) takes the form

$$\partial_{u_s}\partial_v f = 0. \tag{2.30}$$

The general solution is

$$f = c(u_s) + d(v), \tag{2.31}$$

with c and d being arbitrary functions. Thus, in the flat space region, solutions can be any function of u or any function of v, while in the Schwarzschild region they can be any function of u_s or any function of v. Given the relations (2.26) and (2.29), it is clear that any solution in the Schwarzschild region is also a solution in the flat region and vice versa. Once again, the modes are normalized using the scalar product (2.6). There is a complete set of "in" modes that are normalized on $\mathscr{I}^-$ and are given by the expressions

$$f^{\rm in}_{\omega,R} = \frac{e^{-i\omega v}}{\sqrt{4\pi\omega}}, \tag{2.32a}$$

$$f^{\rm in}_{\omega,L} = \frac{e^{-i\omega u}}{\sqrt{4\pi\omega}}. \tag{2.32b}$$

A different complete set of modes consists of subsets that have three different late-time behaviors. Some of the modes

end on $\mathcal{I}_L^+$, others go through the future horizon and end up at the singularity, and the rest end on $\mathcal{I}_R^+$. As with the accelerating mirror, we are interested in those that end up on $\mathcal{I}_R^+$, which we label as "out" modes and which are given by

$$f_\omega^{\rm out} = \frac{e^{-i\omega u_s}}{\sqrt{4\pi\omega}}. \tag{2.33}$$

The other modes we label with the superscripts "left" and "sing."

As in the accelerating mirror case (2.13), the average number of particles found at $\mathcal{I}_R^+$ for a given value of ω if the field is in the "in" state is

$$\langle in|N_\omega^{\rm out}|in\rangle = \langle in|a_\omega^{\rm out\dagger}a_\omega^{\rm out}|in\rangle. \tag{2.34}$$

The expansions of ϕ in terms of these complete sets of modes are

$$\phi = \int_0^\infty d\omega[a_{\omega,R}^{\rm in}f_{\omega,R}^{\rm in} + a_{\omega,R}^{\rm in\dagger}f_{\omega,R}^{\rm in*} + a_{\omega,L}^{\rm in}f_{\omega,L}^{\rm in} + a_{\omega,L}^{\rm in\dagger}f_{\omega,L}^{\rm in*}], \tag{2.35a}$$

$$= \int_0^\infty d\omega[a_\omega^{\rm out}f_\omega^{\rm out} + a_\omega^{\rm out\dagger}f_\omega^{\rm out*} + a_\omega^{\rm left}f_\omega^{\rm left} + a_\omega^{\rm left\dagger}f_\omega^{\rm left*} + a_\omega^{\rm sing}f_\omega^{\rm sing} + a_\omega^{\rm sing\dagger}f_\omega^{\rm sing*}]. \tag{2.35b}$$

In this case, the scalar product $(f_{\omega',R}^{\rm in}, f_\omega^{\rm out}) = 0$, because the "out" modes vanish on $\mathcal{I}_R^-$. Hence,

$$a_\omega^{\rm out} = (\phi, f_\omega^{\rm out}) = \int_0^\infty d\omega'[a_{\omega',L}^{\rm in}(f_{\omega',L}^{\rm in}, f_\omega^{\rm out}) + a_{\omega',L}^{\rm in\dagger}(f_{\omega',L}^{\rm in*}, f_\omega^{\rm out})]. \tag{2.36}$$

If we write

$$f_\omega^{\rm out} = \int_0^\infty d\omega'[\alpha_{\omega\omega'}f_{\omega',L}^{\rm in} + \beta_{\omega\omega'}f_{\omega',L}^{\rm in*}], \tag{2.37}$$

then

$$a_\omega^{\rm out} = \int_0^\infty d\omega'[a_{\omega',L}^{\rm in}\alpha_{\omega\omega'}^* - a_{\omega',L}^{\rm in\dagger}\beta_{\omega\omega'}^*], \tag{2.38}$$

and the Bogolubov coefficients can be obtained from

$$\alpha_{\omega\omega'} = (f_\omega^{\rm out}, f_{\omega',L}^{\rm in}), \tag{2.39a}$$

$$\beta_{\omega\omega'} = -(f_\omega^{\rm out}, f_{\omega',L}^{\rm in*}), \tag{2.39b}$$

while once again the average number of particles is

$$\langle in|N_\omega^{\rm out}|in\rangle = \int_0^\infty d\omega'|\beta_{\omega\omega'}|^2. \tag{2.40}$$

The Cauchy surface we use to compute the Bogolubov coefficients is shown as dotted (and blue) in Fig. 2. It consists of $v = v_0$ plus the part of $\mathcal{I}_R^-$ with $v > v_0$ and all of $\mathcal{I}_L^+$. However, the modes $f_{\omega,R}^{\rm out}$ are nonzero only on the part of the Cauchy surface with $v = v_0$ that is outside the event horizon ($u_s < \infty$, $u < v_H$). Using (2.32b), (2.33), (2.39a), and (2.39b), one finds

$$\alpha_{\omega\omega'} = \frac{1}{4\pi}\int_{-\infty}^{v_H} du e^{-i(\omega-\omega')u}[\kappa(v_H-u)]^{i\omega/\kappa} \times\left[\sqrt{\frac{\omega'}{\omega}} + \sqrt{\frac{\omega}{\omega'}}\left(1+\frac{1}{\kappa(v_H-u)}\right)\right], \tag{2.41a}$$

$$\beta_{\omega\omega'} = \frac{1}{4\pi}\int_{-\infty}^{v_H} du e^{-i(\omega+\omega')u}[\kappa(v_H-u)]^{i\omega/\kappa} \times\left[\sqrt{\frac{\omega'}{\omega}} - \sqrt{\frac{\omega}{\omega'}}\left(1+\frac{1}{\kappa(v_H-u)}\right)\right], \tag{2.41b}$$

where $\kappa = 1/(4M)$ is the surface gravity of the black hole. These equations are identical to Eqs. (2.21) for the mirror trajectory considered in Sec. II A if we make the substitution $u \to v$ and identify the acceleration parameter, κ, in the mirror case, with the surface gravity κ in the black hole case. Thus, the values for $\alpha_{\omega\omega'}$ and $\beta_{\omega\omega'}$ are identical with those in (2.22), and we have found an exact correspondence between the particle production which occurs in $(1+1)$ dimensions for a mirror with trajectory (2.14) and a black hole that forms from the collapse of a null shell along the surface $v = v_0$.

C. (3 + 1)-dimensional spacetime with a collapsing null shell

For a $(3+1)$-dimensional spacetime with a collapsing null shell, the line element inside the shell is that of flat space,

$$ds^2 = -dt^2 + dr^2 + r^2 d\Omega^2, \tag{2.42}$$

and outside the shell is the Schwarzschild metric:

$$ds^2 = -\left(1-\frac{2M}{r}\right)dt_s^2 + \left(1-\frac{2M}{r}\right)^{-1}dr^2 + r^2 d\Omega^2. \tag{2.43}$$

The Penrose diagram is given in Fig. 3.

The radial null coordinates have the same definitions as in the $(1+1)$-dimensional case with those inside the shell given by (2.2) and those outside the shell given by (2.24). The matching of the coordinates across the shell is also the same as in the $(1+1)$-dimensional case with the results given by (2.26) and (2.29).

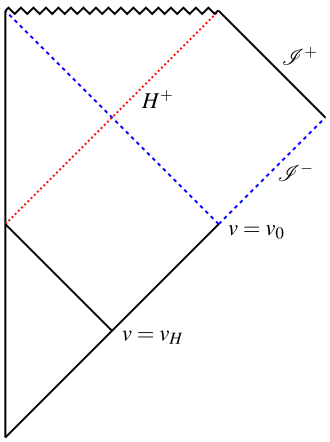

FIG. 3. Penrose diagram for a $(3+1)$-dimensional black hole that forms from the collapse of a null shell along the trajectory $v = v_0$. The horizon, H^+, is the dotted (red) curve. The Cauchy surface used to compute the Bogolubov coefficients is the short-dashed (blue) curve.

The massless minimally coupled scalar field satisfies Eq. (2.3). The field can be expanded in terms of complete sets of modes where the mode functions are written in the general form:

$$f = \frac{Y_{\ell m}(\theta,\phi)}{\sqrt{4\pi\omega}}\frac{\psi(t,r)}{r}. \tag{2.44}$$

Inside the shell, we have the flat-space radial wave equation,

$$-\frac{\partial^2\psi}{\partial t^2} + \frac{\partial^2\psi}{\partial r^2} - V_{\rm eff}(r)\psi = 0, \tag{2.45}$$

while outside the shell, we have the scalar Regge-Wheeler equation

$$-\frac{\partial^2\psi}{\partial t_s^2} + \frac{\partial^2\psi}{\partial r_*^2} - V_{\rm eff}(r)\psi = 0. \tag{2.46}$$

The effective potential is

$$V_{\rm eff} = \left(1 - \frac{2M}{r}\right)\left[\frac{2M}{r^3} + \frac{\ell(\ell+1)}{r^2}\right], \tag{2.47}$$

which can be seen to work in both cases if inside the shell we set $M = 0$.

The modes are normalized using the full three-dimensional version of the scalar product, Eq. (2.6). In the cases we consider, the Cauchy surface consists of either a single null hypersurface or a union of null hypersurfaces, and the integrals are of the forms

$$\int du \int d\Omega r^2 \overleftrightarrow{\partial}_u, \qquad \int dv \int d\Omega r^2 \overleftrightarrow{\partial}_v. \tag{2.48}$$

We consider two complete sets of mode functions. Those for the "in" state are normalized on past null infinity, $\mathscr{I}^-$, and vanish at $r = 0$ inside the shell. Thus, inside the shell, they are the same as the mode functions in flat space in the Minkowski vacuum. On $\mathscr{I}^-$, they are

$$\psi^{\rm in}_{\omega\ell} = e^{-i\omega v}, \tag{2.49}$$

with $0 \le \omega < \infty$. They are, of course, more complicated away from $\mathscr{I}^-$, although there are analytic solutions for them inside the shell. The simplest solution inside the shell is for the mode with $\ell = 0$:

$$\psi^{\rm in}_{\omega 0} = e^{-i\omega v} - e^{-i\omega u}. \tag{2.50}$$

The other complete set of solutions we will consider is a union of two subsets. One subset, of most interest, is normalized on future null infinity, $\mathscr{I}^+$. We label them as "out" modes. On $\mathscr{I}^+$, they are

$$\psi^{\rm out}_{\omega\ell} = e^{-i\omega u_s}, \tag{2.51}$$

where again $0 \le \omega < \infty$. These modes vanish at the future horizon H^+. The other set consists of modes which vanish at $\mathscr{I}^+$ and are nonzero on H^+. We give them the label H^+ and will not be concerned with their normalization here. It is easy to show using the scalar product and a Cauchy surface for the region outside the horizon, which consists of H^+ and $\mathscr{I}^+$, that these two sets of modes are orthogonal.

The expansions for ϕ in terms of the two complete sets of modes are

$$\phi = \int_0^\infty d\omega \sum_{\ell,m} [a^{\rm in}_{\omega\ell m} f^{\rm in}_{\omega\ell m} + a^{\rm in\dagger}_{\omega\ell m} f^{\rm in*}_{\omega\ell m}], \tag{2.52a}$$

$$\phi = \int_0^\infty d\omega \sum_{\ell,m} [a^{\rm out}_{\omega\ell m} f^{\rm out}_{\omega\ell m} + a^{\rm out\dagger}_{\omega\ell m} f^{\rm out*}_{\omega\ell m} + a^{H^+}_{\omega\ell m} f^{H^+}_{\omega\ell m} + a^{H^+\dagger}_{\omega\ell m} f^{H^+*}_{\omega\ell m}]. \tag{2.52b}$$

In this case, the goal is to determine the average number of particles in the "out" state, as a function of ω, ℓ, and m, if the field is in the "in" state. This is given by

$$\langle in|N^{\rm out}_{\omega\ell m}|in\rangle = \langle in|a^{\rm out\dagger}_{\omega\ell m} a^{\rm out}_{\omega\ell m}|in\rangle. \tag{2.53}$$

Using the orthonormality of the mode functions, we find from (2.52) that

$$a^{\rm out}_{\omega\ell m} = (\phi, f^{\rm out}_{\omega\ell m}) = \sum_{\ell',m'} \int_0^\infty d\omega' [a^{\rm in}_{\omega'\ell'm'}(f^{\rm in}_{\omega'\ell'm'}, f^{\rm out}_{\omega\ell m}) + a^{\rm in\dagger}_{\omega'\ell'm'}(f^{\rm in*}_{\omega'\ell'm'}, f^{\rm out}_{\omega\ell m})]. \tag{2.54}$$

If we take the transformation between sets of mode functions to be

$$f^{\rm out}_{\omega\ell m} = \sum_{\ell'm'} \int_0^\infty d\omega' [\alpha_{\omega\ell m\omega'\ell'm'} f^{\rm in}_{\omega'\ell'm'} + \beta_{\omega\ell m\omega'\ell'm'} f^{\rm in*}_{\omega'\ell'm'}], \tag{2.55}$$

then the operators are connected by

$$a^{\rm out}_{\omega\ell m} = \sum_{\ell',m'} \int_0^\infty d\omega' [a^{\rm in}_{\omega'\ell'm'} \alpha^*_{\omega\ell m\omega'\ell'm'} - a^{\rm in\dagger}_{\omega'\ell'm'} \beta^*_{\omega\ell m\omega'\ell'm'}], \tag{2.56}$$

and the expectation value will be

$$\langle in|N^{\rm out}_{\omega\ell m}|in\rangle = \sum_{\ell',m'} \int_0^\infty d\omega' |\beta_{\omega\ell m\omega'\ell'm'}|^2, \tag{2.57}$$

with the Bogolubov coefficients found via

$$\alpha_{\omega\ell m\omega'\ell'm'} = (f^{\rm out}_{\omega\ell m}, f^{\rm in}_{\omega'\ell'm'}), \tag{2.58a}$$

$$\beta_{\omega\ell m\omega'\ell'm'} = -(f^{\rm out}_{\omega\ell m}, f^{\rm in*}_{\omega'\ell'm'}). \tag{2.58b}$$

On any hypersurface where integrals of the form (2.48) are to be computed, the following orthonormality conditions are useful:

$$\int d\Omega Y_{\ell m}(\theta,\phi) Y^*_{\ell'm'}(\theta,\phi) = \delta_{\ell,\ell'}\delta_{m,m'},$$
$$\int d\Omega Y_{\ell m}(\theta,\phi) Y_{\ell'm'}(\theta,\phi) = (-1)^m \delta_{\ell,\ell'}\delta_{m,-m'}. \tag{2.59}$$

It is then possible to show that the Bogolubov coefficients are partially diagonal in the sense that

$$\alpha_{\omega\ell m\omega'\ell'm'} \propto \delta_{\ell,\ell'}\delta_{m,m'}$$
$$\beta_{\omega\ell m\omega'\ell'm'} \propto (-1)^m \delta_{\ell,\ell'}\delta_{m,-m'}, \tag{2.60}$$

and that the average number of particles is

$$\langle in|N^{\rm out}_{\omega\ell m}|in\rangle = \int_0^\infty d\omega' |\beta_{\omega\ell m\omega'\ell(-m)}|^2. \tag{2.61}$$

To compute the Bogolubov coefficients using Eqs. (2.58), it is necessary to choose a Cauchy surface for the spacetime. The choice we make is driven by the fact that we have exact solutions for the mode functions $f^{\rm in}_{\omega\ell m}$ in the region inside the shell and also everywhere on $\mathscr{I}^-$ since that is where these modes are normalized. To get their form in the region outside the shell, it would be necessary either to use a Bogolubov transformation or to solve the partial differential equation (2.46) numerically. The mode functions $f^{\rm out}_{\omega\ell m}$ are normalized on $\mathscr{I}^+$ so we have analytic expressions for them there. They can be computed in the region outside the null shell by separating the functions $\psi_{\omega\ell}$ into

$$\psi_{\omega\ell}(t,r) = e^{-i\omega t}\chi_{\omega\ell}(r), \tag{2.62}$$

and numerically solving the resulting radial equation for $\chi_{\omega\ell}$, which is

$$\frac{d^2\chi_{\omega\ell}}{dr_*^2} + (\omega^2 - V_{\rm eff})\chi_{\omega\ell} = 0. \tag{2.63}$$

However, to extend these solutions to the region inside the null shell to make contact with $f^{\rm in}_{\omega\ell m}$ requires either using a Bogolubov transformation such as Eq. (2.55) or solving the partial differential equation (2.45) numerically. Here we use a Bogolubov transformation and choose the Cauchy surface shown in Fig. 3, which consists of the null surface $v = v_0$ along with the portion of $\mathscr{I}^-$ with $v_0 < v < \infty$.

In a subsequent paper, we intend to numerically solve the mode equation (2.63) when the effective potential is included. In this paper, however, we set $V_{\rm eff} = 0$ and ignore potential barrier effects in order to see what other effects $(3+1)$ dimensions has. Accordingly, inside the shell, the "in" modes are given by Eq. (2.50) for all values of ℓ and m. Similarly, outside the shell the "out" modes are given by

$$\psi^{\rm out}_{\omega\ell} = e^{-i\omega u_s}, \tag{2.64}$$

which are taken to vanish as $u_s \to -\infty$ along $\mathscr{I}^-$ for $v > v_0$. Thus,

$$\alpha_{\omega\ell m\omega'\ell'm'} = -i\frac{\delta_{\ell,\ell'}\delta_{m,m'}}{4\pi\sqrt{\omega\omega'}} \int_{-\infty}^{v_H} du e^{-i\omega u_s} \overleftrightarrow{\partial}_u (e^{i\omega' v_0} - e^{i\omega' u}), \tag{2.65a}$$

$$\beta_{\omega\ell m\omega'\ell'm'} = i(-1)^m \frac{\delta_{\ell,\ell'}\delta_{m,-m'}}{4\pi\sqrt{\omega\omega'}} \times \int_{-\infty}^{v_H} du e^{-i\omega u_s} \overleftrightarrow{\partial}_u (e^{-i\omega' v_0} - e^{-i\omega' u}). \tag{2.65b}$$

Note that the terms in the integrands with factors of $e^{\pm i\omega' v_0}$ are total derivatives and can be integrated trivially. Because $e^{\pm i\omega u_s}$ effectively vanishes at $u_s = \pm\infty$, these terms vanish also. The result is that

$$\alpha_{\omega\ell m\omega'\ell'm'} = -\frac{\delta_{\ell,\ell'}\delta_{m,m'}}{4\pi}\int_{-\infty}^{v_H} du e^{-i(\omega-\omega')u}[\kappa(v_H-u)]^{i\omega/\kappa}\left[\sqrt{\frac{\omega'}{\omega}}+\sqrt{\frac{\omega}{\omega'}}\left(1+\frac{1}{\kappa(v_H-u)}\right)\right], \tag{2.66a}$$

$$\beta_{\omega\ell m\omega'\ell'm'} = \frac{(-1)^{m+1}\delta_{\ell,\ell'}\delta_{m,-m'}}{4\pi}\int_{-\infty}^{v_H} du e^{-i(\omega+\omega')u}[\kappa(v_H-u)]^{i\omega/\kappa}\left[\sqrt{\frac{\omega'}{\omega}}-\sqrt{\frac{\omega}{\omega'}}\left(1+\frac{1}{\kappa(v_H-u)}\right)\right]. \tag{2.66b}$$

The expression for $\alpha_{\omega\ell m\omega'\ell'm'}$ differs from the $(1+1)$-dimensional case in (2.41a) by the factor of $-\delta_{\ell,\ell'}\delta_{m,m'}$, and the expression for $\beta_{\omega\ell m\omega'\ell'm'}$ differs from the $(1+1)$-dimensional case in (2.41b) by the factor of $(-1)^{m+1}\delta_{\ell,\ell'}\delta_{m,-m'}$.

As mentioned in the Introduction, Massar and Parentani [4] have computed the Bogolubov coefficients for the case of a null shell collapsing to form a black hole. Their computation was for the s-wave sector in the $(3+1)$-dimensional case when the effective potential is ignored. Thus it was the same as the case done in this subsection. By restricting to the s-wave sector, they effectively considered the $(1+1)$-dimensional case as well. However, because they began with the $(3+1)$-dimensional case, their mode functions vanish at $r=0$ inside the shell. In our separate $(1+1)$-dimensional model, we make no such assumption and instead have modes arising from $\mathcal{I}_L^-$. Despite that difference, both models yield the same amount of particle production. (Note that there is a missing normalization factor of $8M$ in Eq. (10) of [4].)

III. TIME- AND FREQUENCY-RESOLVED SPECTRA

To investigate the time dependence of the particle production rate, we construct localized wave packets of a form originally used by Hawking [1] and which were used by us in Ref. [8] to examine a set of accelerating mirror models. When this constructive process is applied to mode functions of definite frequency, the resulting packets form a complete orthonormal set that subdivides (and provides a degree of localization) within both the time and frequency domains. Following [14], a given mode packet is defined as

$$f_{jn}^{\text{out}} \equiv \frac{1}{\sqrt{\epsilon}}\int_{j\epsilon}^{(j+1)\epsilon} d\omega\, e^{2\pi i\omega n/\epsilon} f_\omega^{\text{out}}. \tag{3.1}$$

A packet with index j covers the range of frequencies $j\epsilon \le \omega \le (j+1)\epsilon$. Since the definite frequency "out" modes approach $\mathcal{I}_R^+$ with the behavior $f_\omega^{\text{out}} \sim e^{-i\omega u_s}$, a packet with index n covers the approximate time range $(2\pi n-\pi)/\epsilon \lesssim u_s \lesssim (2\pi n+\pi)/\epsilon$. We can write

$$\beta_{jn,\omega'} \equiv -(f_{jn}^{\text{out}}, f_{\omega'}^{\text{in}*}). \tag{3.2}$$

Using Eq. (3.1) and interchanging the order of integration gives

$$\beta_{jn,\omega'} = \frac{1}{\sqrt{\epsilon}}\int_{j\epsilon}^{(j+1)\epsilon} d\omega e^{2\pi i\omega n/\epsilon}\beta_{\omega\omega'}. \tag{3.3}$$

Then the quantity

$$\langle \text{in}|N_{jn}^{\text{out}}|\text{in}\rangle \equiv \int_0^\infty d\omega'|\beta_{jn,\omega'}|^2 \tag{3.4}$$

can be thought of as giving the average number of particles detected by a particle detector that was sensitive to the frequency range $j\epsilon \le \omega \le (j+1)\epsilon$ and was turned on during the time period $(2\pi n-\pi)/\epsilon \lesssim u_s \lesssim (2\pi n+\pi)/\epsilon$. Note that the value of $\langle N_{jn}\rangle$ is the same for both the mirror and the $(1+1)$-dimensional spacetime with a collapsing null shell since the values of $\beta_{\omega\omega'}$ are the same in those cases.

A similar expression works for the $(3+1)$-dimensional spacetime with a collapsing null shell for given values of ℓ and m. If, as in the previous section, we neglect V_{eff}, then the value of β for given ω and ω' is the same for all ℓ and m. Thus summing over ℓ and m results in an infinite number of particles for each value of j and n. If the mode equation is solved by including V_{eff}, then the number of particles for each value of j and n will be finite [14] (a case we will discuss elsewhere).

If Eq. (2.22b) is substituted into Eq. (3.3), then in the late-time, large-n limit, one can see that the dominant contribution to the integral comes from values of ω' for which the arguments of the oscillating exponentials cancel or nearly cancel and which, therefore, satisfy the condition $\omega' \gg \omega$. In this limit,

$$|\beta_{\omega\omega'}|^2 \sim \frac{1}{2\pi\kappa\omega'}\frac{1}{e^{2\pi\omega/\kappa}-1}, \tag{3.5}$$

and one sees that there is a thermal distribution of particles with temperature $T=\kappa/2\pi$. Thus, the radiation will asymptotically approach a thermal distribution at the black hole temperature. Such a late-time thermal distribution was found for black hole radiation in [1] and for mirrors with a particular class of asymptotically null trajectories in [3].

To compare the exact results with a thermal spectrum, it is useful to write the thermal spectrum in terms of packets.

This has been done in [8] for a mirror trajectory studied by Carlitz and Willey [6] in which the particle production is always in a thermal distribution. The trajectory is [8]

$$z(t) = -t - \frac{1}{\kappa} W(e^{-2\kappa t}), \tag{3.6}$$

and the relevant Bogolubov coefficient is

$$\beta_{\omega\omega'} = \frac{1}{4\pi\sqrt{\omega\omega'}} \left[-\frac{2\omega}{\kappa} e^{-\pi\omega/2\kappa} \left(\frac{\omega'}{\kappa}\right)^{-i\omega/\kappa} \Gamma\left(\frac{i\omega}{\kappa}\right) \right]. \tag{3.7}$$

Substituting Eq. (3.7) into Eq. (3.3) and then into Eq. (3.4) yields

$$\langle N_{jn} \rangle = \frac{1}{\epsilon} \int_{j\epsilon}^{(j+1)\epsilon} \frac{d\omega}{e^{2\pi\omega/\kappa} - 1} = \frac{\kappa}{2\pi\epsilon} \log\left[\frac{e^{\frac{2\pi(j+1)\epsilon}{\kappa}} - 1}{e^{\frac{2\pi j\epsilon}{\kappa}} - 1} \right] - 1. \tag{3.8}$$

Note that the packets depend on the frequency parameters ϵ and j but not the time parameter n, as would be expected if the particles are always produced in a constant-temperature thermal distribution. Note also that the infrared divergence in Eq. (3.7) results in a divergence in the $j = 0$ bin in Eq. (3.8). Since all real particle detectors have infrared cutoffs, for simplicity we simply ignore the $j = 0$ bin when making comparisons with our results for the trajectory (2.14).

An interesting balance in time and frequency resolution occurs for

$$\epsilon = \frac{\kappa}{2\pi} \log\left(\frac{1 + \sqrt{5}}{2} \right) = T \operatorname{csch}^{-1}(2). \tag{3.9}$$

With this packet width, one can show, using Eq. (3.8), that a thermal distribution has[2]

$$\sum_{j=1}^{\infty} \langle N_j \rangle = \langle N_{j=1} \rangle + \sum_{j=2}^{\infty} \langle N_j \rangle = 1 + 1 = 2. \tag{3.10}$$

It is possible, for both the particle production from a mirror following the Carlitz-Willey trajectory (3.6) and that from a mirror following our accelerating mirror trajectory (2.14), to scale out the dependence of $\langle N_{jn} \rangle$ on κ by working with the following dimensionless quantities:

$$x \equiv \frac{\omega}{\kappa}, \tag{3.11a}$$

$$\bar{\epsilon} \equiv \frac{\epsilon}{\kappa}, \tag{3.11b}$$

$$\bar{v}_H \equiv \kappa v_H. \tag{3.11c}$$

[2]The argument of the logarithm is of course the golden ratio. Its significance here is simply that it results in the sum (3.10).

Using Eq. (2.22b), we find for the trajectory (2.14) that

$$\begin{aligned} \langle N_{jn} \rangle = \frac{1}{4\pi^2 \bar{\epsilon}} \int_0^{\infty} dx' \int_{j\bar{\epsilon}}^{(j+1)\bar{\epsilon}} dx_1 \\ \times \int_{j\bar{\epsilon}}^{(j+1)\bar{\epsilon}} dx_2 e^{i(2\pi n/\bar{\epsilon} - \bar{v}_H)(x_1 - x_2)} e^{-\pi(x_1 + x_2)/2} \\ \times x' \sqrt{x_1 x_2} (x_1 + x')^{-ix_1 - 1} (x_2 + x')^{ix_2 - 1} \\ \times \Gamma(ix_1)\Gamma(-ix_2). \end{aligned} \tag{3.12}$$

For the other mirror trajectories studied in [8], which were all inertial at late times, it was found that choosing a small enough value for ϵ and, thus, a small enough range for each value of j in terms of ω gives fine-grained frequency resolution but coarse-grained time resolution. Similarly, choosing a large enough value of ϵ results in a fine-grained time resolution but coarse-grained frequency resolution. It is not possible, of course, to get arbitrary fine-grained simultaneous time and frequency resolution. However, for the asymptotically inertial trajectories studied in [8] attempts to obtain any significant degree of simultaneous time and frequency resolution were not successful. As shown below, for the asymptotically null trajectory (2.14) we have had some success in locating an optimal compromise in time and frequency resolution.

We begin by illustrating the time dependence of the particle production rate by choosing the relatively large number $\bar{\epsilon} = 1$. Because any realistic particle detector will have an infrared frequency cutoff, we shall impose one by only considering bins with $j \geq 1$. For this value of $\bar{\epsilon}$ and for the Bogolubov coefficient (2.22b), we find that most of the particles are in the bin with $j = 1$. The time evolution of the average number of particles detected in this bin is given in Fig. 4 for the case $v_H = 0$. It can be seen from this figure that the particle production rate monotonically increases to its thermal value.

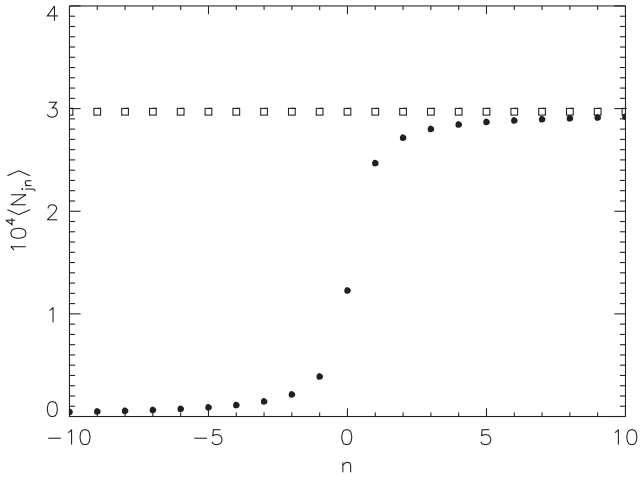

FIG. 4. Average number of particles produced in the $j = 1$ frequency bin as a function of the time parameter n for $\bar{\epsilon} = 1$. The open boxes correspond to the thermal distribution (3.8).

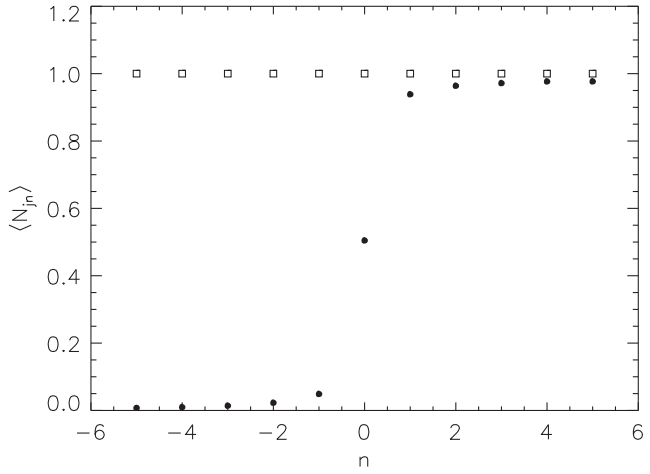

FIG. 5. Average number of particles produced in the $j = 1$ frequency bin as a function of the time parameter n for the packet width in Eq. (3.9). The open boxes correspond to the thermal distribution (3.8).

What can also be seen from Fig. 4 is the very small value that $\langle N_{jn} \rangle$ has. This means that the actual amount of particle production that one would expect in a specific instance would be very low. This is related to the fact that, even at late times, the flux of radiation due to black hole evaporation is very sparse [15]. Similar results were found for the asymptotically inertial mirror trajectories in [8].

To investigate the frequency spectrum, we can make use of the specific packet width in Eq. (3.9), which is small enough to provide some frequency resolution. First, however, in Fig. 5 we show the time dependence of the particle number for the $j = 1$ bin. It is clear that the time resolution is not as good as for the case $\bar{\epsilon} = 1$ in Fig. 4. The frequency resolution is shown for three different times in Fig. 6. It is seen that we have reasonably fine-grained frequency resolution for the time parameters $n = -1$, 0, 1, while the amount of particle production in a given time interval is larger in a low-frequency bin than a high-frequency bin.

The increase in particle production is monotonic with no significant feature in the particle spectrum and production rate near the time of black hole formation in contrast to the initial burst of particles seen for the mirror trajectory in [9]. The approach to a thermal distribution is expected since the mirror trajectory is asymptotically null and, in the collapsing null shell case, the backreaction of the black hole radiation on the spacetime geometry is ignored. In contrast, for the asymptotically inertial trajectories studied in [8,9], one finds a peak in the amount of particle production followed by a steady decline.

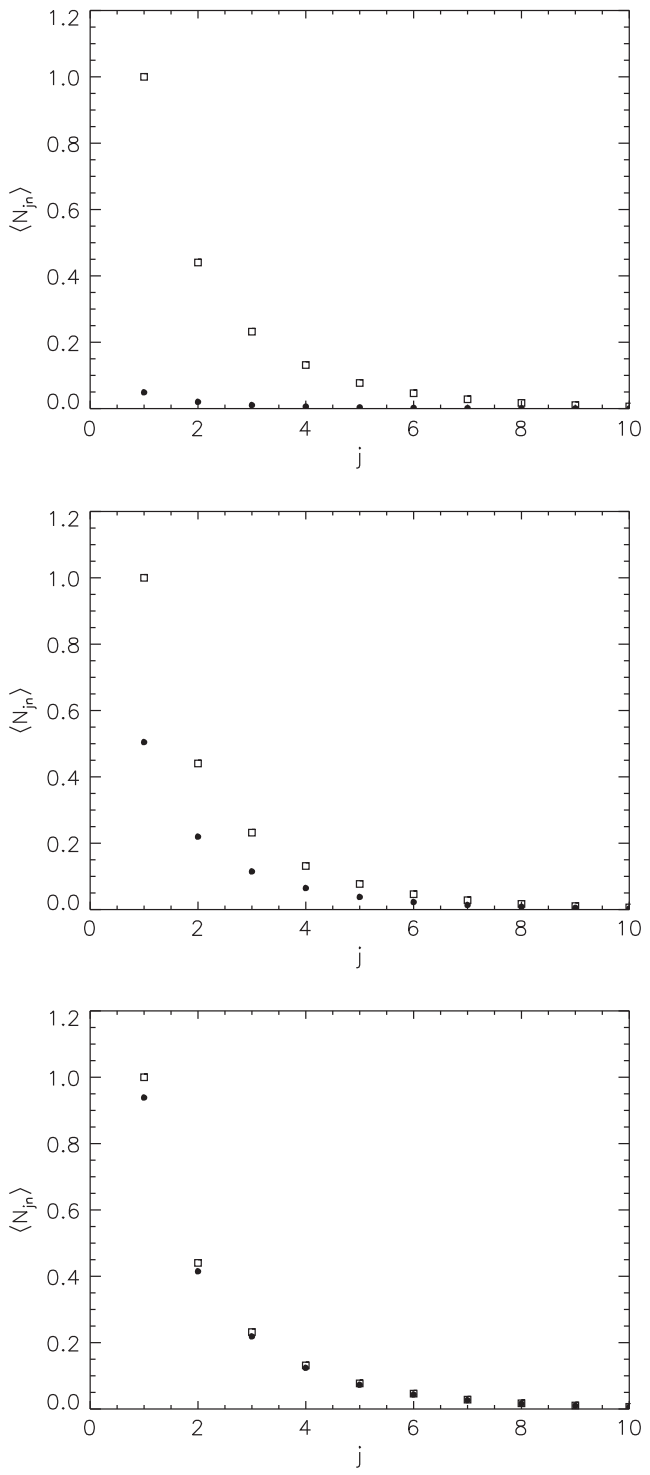

FIG. 6. Plotted are the frequency spectra for the average number of particles produced with the packet width in Eq. (3.9). From top to bottom, the plots are for the values of the time parameter $n = -1$, 0, 1. The open boxes correspond to the thermal distribution (3.8).

IV. STRESS-ENERGY TENSOR

Here we compute the stress-energy tensor for the accelerating mirror spacetime. The general form of the energy flux for any mirror trajectory as a function of time u is [2]

$$F(u) \equiv \langle T_{uu} \rangle = \frac{1}{24\pi}\left(\frac{3}{2}\frac{p''^2}{p'^2} - \frac{p'''}{p'}\right), \tag{4.1}$$

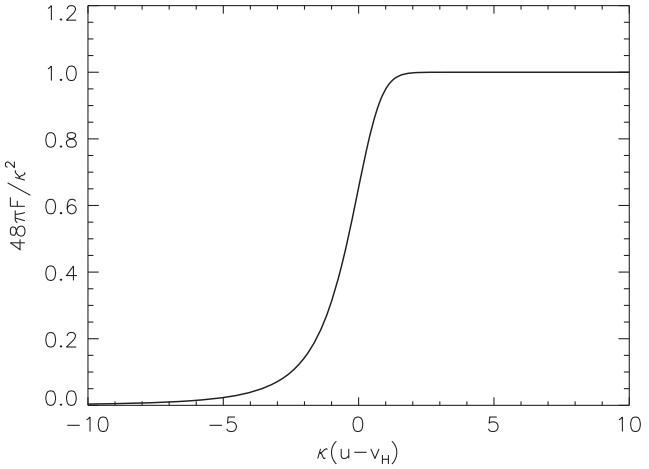

FIG. 7. Energy flux of a quantized massless minimally coupled scalar field for the accelerating mirror spacetime. At late times, the flux approaches its asymptotic value in Eq. (4.3).

where the primes are derivatives with respect to u.[3] The energy flux for the trajectory (2.14) is

$$F(u) = \frac{\kappa^2}{48\pi}\frac{[4W(e^{-\kappa(u-v_H)})+1]}{[W(e^{-\kappa(u-v_H)})+1]^4}. \tag{4.2}$$

It is shown in Fig. 7. Note that, unlike the case of mirror trajectories which are asymptotically inertial, there is no negative energy flux in this case. In the late-time limit, the flux approaches the thermal value

$$F = \frac{\kappa^2}{48\pi}, \tag{4.3}$$

which is the value at all times for the case of a mirror following the Carlitz-Willey trajectory (3.6).

An interesting question is whether there is some way to characterize the nonthermal epoch beyond the observation that the approach to a thermal state is monotonic for both the particle production and the stress-energy tensor. One way to do so is to look at how quickly a given quantity changes. The rate, $F'(u)$, at which the energy flux changes is

$$F'(u) = \frac{\kappa^3}{4\pi}\frac{[W(e^{-\kappa(u-v_H)})]^2}{[W(e^{-\kappa(u-v_H)})+1]^6}. \tag{4.4}$$

The particular time, $u_{\max}$, at which the rate $F'(u)$ reaches its maximum value, is important because that is the time at which the system is furthest away from both its late-time thermal emission and its early-time zero emission. It is

$$\kappa(u_{\max} - v_H) = \ln 2 - \frac{1}{2} \approx 0.19. \tag{4.5}$$

It is interesting to note that this is the same time at which $|z''(u)|$ and $|p''(u)|$ reach their maximum values. This time is also comparable to the time at which the change in the particle production rate is a maximum. This can be seen from Fig. 4 to be at $n \approx 0$, which corresponds to $u \approx 0$. Recall that the time corresponding to n is approximately $u = 2\pi n/\epsilon$. For $u > u_{\max}$, the rate of change of the flux falls off rapidly so there is an asymmetry in the growth of the flux. This can be seen from the fact that, at $u = u_{\max}$, the flux is $16/27 \approx 60\%$ of its asymptotic value. This asymmetry is also reflected in the particle creation rate, lending support to the notion that, in this case, the particles carry the energy [16].

V. CONCLUSIONS

We have displayed an exact correspondence between the particle production in $(1+1)$ dimensions that occurs for a mirror in flat space with the trajectory (2.14) and the particle production that occurs when a black hole forms from gravitational collapse of a null shell. There is also a correspondence in the case of a null shell collapsing to form a black hole in $(3+1)$ dimensions if the effective potential in the mode equation is ignored.

We have used wave packets of the form (3.1) to investigate the time dependence of the particle production rate in the $(1+1)$-dimensional cases. We found that the particle production rate increases monotonically with time. We have also computed the stress-energy tensor $\langle T_{ab}\rangle$ for the scalar field in the case of the accelerating mirror. The rate of change of the particle production mimics the rate of change of energy production in time. With a relativity slow increase and fast decrease, the rate of change of energy-particle flux peaks at a maximum time that corresponds to the most nonthermal, out-of-equilibrium time of the system. The fact that the rate loss is greater than the rate gain points to an asymmetry in the approach to equilibrium. The energy flux is approximately 60% of its maximum equilibrium value at the time when the system is the most out of equilibrium.

The monotonic increase in particle production underscores the relatively calm approach to equilibrium. There are no characteristic imprints to identify the energy flux in the particle emission. However, the peak nonthermal time can be identified and the rate of change of energy flux is mirrored in the rate of change of particle production: clear signatures of the particle-energy coupling during the nonequilibrium phase.

ACKNOWLEDGMENTS

M. R. R. G. thanks Yen Chin Ong, Don Page, and William Unruh for clarifying some ideas. P. R. A. would

[3]This can also be expressed in terms of the rapidity $\eta(u) \equiv \tanh^{-1}[\dot{z}(t_m(u))] = \frac{1}{2}\ln p'(u)$. The result is $12\pi F(u) = [\eta'(u)]^2 - \eta''(u)$.

like to thank Renaud Parentani, and P. R. A. and C. R. E. would like to thank Alessandro Fabbri and Amos Ori for helpful conversations. This work was supported in part by the National Science Foundation under Grants No. PHY-0856050, No. PHY-1308325, and No. PHY-1505875 to Wake Forest University (WFU), and No. PHY-1506182 to the University of North Carolina, Chapel Hill. C. R. E. acknowledges support from the Bahnson Fund at the University of North Carolina, Chapel Hill. Some of the plots were generated on the WFU DEAC cluster; we thank the WFU Provost's Office and Information Systems Department for their generous support.

[1] S. Hawking, Commun. Math. Phys. **43**, 199 (1975).
[2] S. A. Fulling and P. C. W. Davies, Proc. R. Soc. A **348**, 393 (1976).
[3] P. C. W. Davies and S. A. Fulling, Proc. R. Soc. A **356**, 237 (1977)
[4] S. Massar and R. Parentani, Phys. Rev. D **54**, 7444 (1996).
[5] M. R. R. Good, Ph.D. thesis, University of North Carolina, 2011, UMI Dissertations ISBN: 9781124942285.
[6] R. D. Carlitz and R. S. Willey, Phys. Rev. D **36**, 2327 (1987).
[7] W. R. Walker and P. C. W. Davies, J. Phys. A **15**, L477 (1982).
[8] M. R. R. Good, P. R. Anderson, and C. R. Evans, Phys. Rev. D **88**, 025023 (2013).
[9] M. R. R. Good and Y. C. Ong, J. High Energy Phys. 07 (2015) 145.
[10] P. R. Anderson, M. R. R. Good, and C. R. Evans, arXiv:1507.03489.
[11] M. R. R. Good, P. R. Anderson, and C. R. Evans, arXiv:1507.05048.
[12] M. R. R. Good, in *LeCosPA Symposium Proceedings*, Taipei, 2015, arXiv:1602.00683.
[13] C. W. Misner, K. S. Thorne, and J. A. Wheeler, *Gravitation* (Freeman, San Francisco, 1973).
[14] A. Fabbri and J. Navarro-Salas, *Modeling Black Hole Evaporation* (Imperial College Press, London, 2005).
[15] See e.g. F. Gray, S. Schuster, A. Van-Brunt, and M. Visser, Classical Quantum Gravity **33**, 115003 (2016), and references therein.
[16] W. R. Walker, Phys. Rev. D **31**, 767 (1985).